

# **Eocene magmatism in the Himalaya: A response to lithospheric flexure during early Indian collision?**

Lin Ma et al.

## **Data Depository 1 (Texts)**

### **1 Methods**

#### **1.1 Zircon U-Pb age analyses**

U-Pb analyses were carried out using the Cameca IMS-1280HR ion probe at the State Key Laboratory of Isotope Geochemistry (SKLaBIG), Guangzhou Institute of Geochemistry, Chinese Academy of Sciences (GIG CAS). Analytical procedures are similar to those described by [Li et al. \(2009\)](#). An  $O_2^-$  primary ion beam with an intensity of  $\sim 10$  nA was accelerated at -13kV. The ellipsoidal spot was about  $20 \times 30$   $\mu m$  in size. The aperture illumination mode (Kohler illumination) was used with a 200  $\mu m$  primary beam mass filter (PBMF) aperture to produce even sputtering over the entire analyzed area. In the secondary ion beam optics, a 60 eV energy window was used, together with a mass resolution of  $\sim 5400$  to separate  $Pb^+$  peaks from isobaric interferences. Rectangular lenses were activated in the secondary ion optics to increase the transmission at high mass resolution. A single electron multiplier was used in ion-counting mode to measure secondary ion beam intensities by the peak jumping sequence: 196 ( $^{90}Zr^{216}O$ , matrix reference), 200 ( $^{92}Zr^{216}O$ ), 200.5 (background), 203.81 ( $^{94}Zr^{216}O$ , for mass calibration), 203.97 (Pb), 206 (Pb), 207 (Pb), 208 (Pb), 209 ( $^{177}Hf^{16}O_2$ ), 238 (U), 248 ( $^{232}Th^{16}O$ ), 270 ( $^{238}U^{16}O_2$ ), and 270.1 (reference mass). The integration time for these mass are 1.04, 0.56, 4.16, 0.56, 6.24, 4.16, 6.24, 2.08, 1.04, 2.08, 2.08, 2.08, and 0.24 s, respectively. Each measurement consisted of seven cycles, and the total analytical time per measurement was  $\sim 12$  minutes.

Zircon U–Th–Pb isotopic ratios were corrected using the standard zircon Plešovice (337.1 Ma) ([Sláma et al., 2008](#)) based on an observed linear relationship between  $ln$

( $^{206}\text{Pb}/^{238}\text{U}$ ) and  $\ln(^{238}\text{U}^{16}\text{O}_2/^{238}\text{U})$  (Whitehouse et al., 1997). Common Pb is assumed largely to have derived from laboratory contamination introduced during sample preparation (Ireland and Williams, 2003). Measured compositions were corrected for common Pb using  $^{207}\text{Pb}$ -based method with common lead isotope composition of  $^{207}\text{Pb}/^{206}\text{Pb}$  ratio anchored at 0.8356. In this study, we analyzed 11 Qinghu grains yielding a weighted mean age of  $159.0 \pm 1.5$  Ma, which is identical to the recommended value of  $159.5 \pm 0.2$  Ma within analytical uncertainties (Li et al., 2013).

## 1.2 Whole-rock element geochemical analyses

Rock samples were first examined by optical microscopy. Selected whole-rock samples were then sawn into small chips and ultrasonically cleaned in distilled water with  $< 3\%$   $\text{HNO}_3$  and then in distilled water alone, and subsequently dried and handpicked to remove visible contamination. The rocks were crushed and ground in a tungsten carbide ring mill, and the resulting powder was used for analyses of major and trace elements, and Sr–Nd isotopes, at SKLaBIG, GIG CAS. Major–element oxides were analyzed on fused glass beads using a Rigaku RIX 2000 X-ray fluorescence spectrometer at SKLaBIG, GIG–CAS. Calibration lines used in quantification were produced by bivariate regression of data from 36 reference materials encompassing a wide range of silicate compositions (Li et al., 2005), and analytical uncertainties are between 1% and 5%. Trace elements were analyzed by ICP-MS, using a Perkin–Elmer Sciex ELAN 6000 instrument at SKLaBIG, GIG CAS. Analytical procedures are the same as these described by Li et al. (2002). Repeated ICP-MS runs gave  $< 3\%$  RSD (relative standard deviation) for most element abundances in reference materials.

## 1.3 Whole-rock Sr–Nd isotope geochemical analyses

Sr and Nd isotopic compositions of selected samples were determined using a MC–ICP-MS at SKLaBIG, GIG–CAS. Analytical procedures are similar to those described in Wei et al. (2002) and Li et al. (2004). The  $^{87}\text{Sr}/^{86}\text{Sr}$  ratio of the NBS987 standard and  $^{143}\text{Nd}/^{144}\text{Nd}$  ratio of the Shin Etsu JNdi–1 standard measured were  $0.710271 \pm 6$  ( $2\sigma$ )

and  $0.512096 \pm 3$  ( $2\sigma$ ), respectively. All measured  $^{143}\text{Nd}/^{144}\text{Nd}$  and  $^{86}\text{Sr}/^{88}\text{Sr}$  ratios were corrected for fractionation using ratios of  $^{146}\text{Nd}/^{144}\text{Nd} = 0.7219$  and  $^{86}\text{Sr}/^{88}\text{Sr} = 0.1194$ , respectively. The BHVO-2 and JB-3 reference materials were run as unknowns and yielded  $^{87}\text{Sr}/^{86}\text{Sr}$  and  $^{143}\text{Nd}/^{144}\text{Nd}$  ratios of  $0.703481 \pm 11$ ,  $0.703438 \pm 8$ , and  $0.512979 \pm 22$  and  $0.513044 \pm 5$ , respectively. All these are in good agreement with the recommended  $^{87}\text{Sr}/^{86}\text{Sr}$  and  $^{143}\text{Nd}/^{144}\text{Nd}$  ratios of  $0.703475 \pm 17$  (Weis and Kieffer, 2005),  $0.703428 \pm 10$  (Orihashi et al., 1998), and  $0.512986 \pm 8$  (Weis et al., 2005) and  $0.513035 \pm 9$  (Iizumi et al., 1995).

#### 1.4 Zircon O isotope analyses

Measurements of zircon O isotopes were conducted using the Cameca IMS 1280HR large-radius SIMS (Secondary Ion Mass Spectroscopy) at the SKLaBIG, GIG CAS. Analytical procedures are the same as those described by Li et al. (2010a). The  $\text{Cs}^+$  primary ion beam was accelerated at 10 kV, with an intensity of ca. 2 nA (Gaussian mode with a primary beam aperture of 200  $\mu\text{m}$  to reduce aberrations) and rastered over a 10  $\mu\text{m}$  area. The spot is about 20  $\mu\text{m}$  in diameter (10  $\mu\text{m}$  beam diameter + 10  $\mu\text{m}$  raster).

A normal-incidence electron flood gun was used to compensate for sample charging during analysis with homogeneous electron density over a 100  $\mu\text{m}$  oval area. Negative secondary ions were extracted with a -10 kV potential. The field aperture was set to 5000  $\mu\text{m}$ , and the transfer-optics magnification was adjusted to give a field of view of 125  $\mu\text{m}$  (FA=8000). A 30 eV energy slit width was used, and its mechanical positions were controlled before starting the analysis (5 eV gap, -500 digits with respect to the maximum). The entrance slit width was  $\sim 120$   $\mu\text{m}$ , and the exit slit width was 500 microns for multicollector Faraday cups (FCs) for  $^{16}\text{O}$  and  $^{18}\text{O}$  is 500  $\mu\text{m}$  (MRP = 2500). The intensity of  $^{16}\text{O}$  was typically  $1 \times 10^9$  cps. Oxygen isotopes were measured in multi-collector mode using two off-axis Faraday cups. The NMR (Nuclear Magnetic Resonance) probe was used for magnetic field control with stability better than 2.5 ppm over 16 h on mass 17. One analysis takes  $\sim 4$  minutes, consisting of pre-sputtering ( $\sim 120$

s), automatic beam centering (~60 s) and integration of oxygen isotopes (10 cycles×4 s, total 40 s). Uncertainties on individual analyses are reported at a 2σ level. With low noise on the two FC amplifiers, the internal precision of a single analysis is generally better than 0.3‰ (2σ) for <sup>18</sup>O/<sup>16</sup>O ratio. Values of δ<sup>18</sup>O are standardized to Vienna Standard Mean Ocean Water compositions (VSMOW) and reported in standard per mil notation.

The instrumental mass fractionation factor (IMF) is corrected using the Penglai zircon standard (Li et al., 2010b). Measured <sup>18</sup>O/<sup>16</sup>O is normalized using VSMOW, then corrected for the instrumental mass fractionation factor (IMF) as follows:

$$(\delta^{18}\text{O})_{\text{M}} = ((^{18}\text{O}/^{16}\text{O})_{\text{M}} / 0.0020052 - 1) \times 1000 (\text{‰})$$

$$\text{IMF} = (\delta^{18}\text{O})_{\text{M(standard)}} - (\delta^{18}\text{O})_{\text{VSMOW}}$$

$$\delta^{18}\text{O}_{\text{sample}} = (\delta^{18}\text{O})_{\text{M}} + \text{IMF}$$

Fifteen measurements of the Qinghu zircon standard during the course of this study yielded a weighted mean of δ<sup>18</sup>O = 5.57 ± 0.4 ‰, which is identical within errors to the reported value of 5.4 ± 0.2 ‰ (Li et al., 2013).

## 2 Effects of alteration, and magma chamber process

The Gyantse mafic rocks show high and variable loss on ignition (LOI = 2.1–9.1), suggesting potential impact of alteration on element mobility. Given that Zr is a relatively immobile element during sub-solidus alteration, correlations between elements and Zr can be used to assess the mobility of elements during post-magmatic processes. The scattered distribution of elements such as Rb, Ba and Sr (Fig. DR1a) indicates probable significant elemental mobility. In contrast, the high field strength elements (HFSE), such as Nb and Hf and the rare earth elements (REEs) show a good correlation with Zr (Fig. DR1b-f), implying that these elements

were essentially immobile during alteration. Thus, only the immobile elements are used to assess sources and petrogenetic processes as part of this study.

Crustal assimilation is almost inevitable for mantle-derived melts during their ascent through continental crust or their evolution within a crustal magma chamber (e.g., [Castillo et al., 1999](#)). The negative  $\epsilon\text{Nd}(t)$  (-2.7 to -2.0) of the Gyantse mafic dykes suggest the possibility of crustal assimilation. However, there is no correlation of Nd isotopes and Nb/La ratios with MgO, suggesting that negligible crustal contamination has occurred in these rocks ([Fig. DR1g-i](#)). Moreover, the mantle-like zircon O isotopic compositions ( $\delta^{18}\text{O}$  of 5.1‰–6.4‰) and moderate-high MgO contents (5.0–13.9 wt.%) of the mafic dykes suggest origin of mantle peridotite with insignificant crustal contamination ([Fig. DR3](#)).

The variable major and trace element compositions of the Gyantse mafic dykes indicate varying but generally low degrees of fractional crystallization and/or crystal accumulation during their formation. All but sample 13JZ11-3 show insignificant effects of crystal accumulation because: (1) outcrops do not show layered structures, and textural evidence for crystal accumulation has not been observed in field and thin sections ([Fig. DR2](#)); (2) slight Eu anomalies ( $\text{Eu}/\text{Eu}^* = 0.85\text{--}1.10$ ) contrast with the pronounced positive Eu anomaly in mafic rocks with cumulate plagioclase ([Fig. 2](#)); (3) the lack of correlation between  $\text{SiO}_2$  and MgO also suggest insignificant accumulation ([Fig. DR1j-l](#)). Thus, the variable major and trace element compositions of the Gyantse mafic dykes indicate that they underwent low degrees of fractional crystallization ([Fig. DR1j-l](#)).

## References Cited

- Castillo, P. R., Janney, P. E., and Solidum, R. U., 1999, Petrology and geochemistry of Camiguin Island, southern Philippines: insights to the source of adakites and other lavas in a complex arc setting: *Contributions to Mineralogy and Petrology*, v. 134, p. 33-51.
- Iizumi, S., Morris, P. A., and Sawada, Y., 1995, Nd isotope data for GSJ reference samples JB-1a, JB-3 and JG-1a and the La Jolla standard: *Mem. Fac. Sci. Shimane Univ.*, v. 29, p. 73-76.
- Ireland, T. R., and Williams, I. S., 2003, Considerations in zircon geochronology by SIMS: *Reviews in mineralogy and geochemistry*, v. 53, no. 1, p. 215-241.
- Li, X.-H., Li, W.-X., Li, Q.-L., Wang, X.-C., Liu, Y., and Yang, Y.-H., 2010a, Petrogenesis and tectonic significance of the ~ 850 Ma Gangbian alkaline complex in South China: evidence from in situ zircon U–Pb dating, Hf–O isotopes and whole-rock geochemistry: *Lithos*, v. 114, no. 1, p. 1-15.
- Li, X., Tang, G., Gong, B., Yang, Y., Hou, K., Hu, Z., Li, Q., Liu, Y., and Li, W., 2013, Qinghu zircon: A working reference for microbeam analysis of U–Pb age and Hf and O isotopes: *Chinese Science Bulletin*, v. 58, no. 36, p. 4647-4654.
- Li, X. H., Liu, D., Sun, M., Li, W. X., Liang, X. R., and Liu, Y., 2004, Precise Sm–Nd and U–Pb isotopic dating of the supergiant Shizhuyuan polymetallic deposit and its host granite, SE China: *Geological Magazine*, v. 141, no. 2, p. 225.
- Li, X. H., Liu, Y., Li, Q. L., Guo, C. H., and Chamberlain, K. R., 2009, Precise determination of Phanerozoic zircon Pb/Pb age by multicollector SIMS without external standardization: *Geochemistry, Geophysics, Geosystems*, v. 10, no. 4.
- Li, X. H., Long, W. G., Li, Q. L., Liu, Y., Zheng, Y. F., Yang, Y. H., Chamberlain, K. R., Wan, D. F., Guo, C. H., and Wang, X. C., 2010b, Penglai zircon megacrysts: a potential new working reference material for microbeam determination of Hf–O isotopes and U–Pb age: *Geostandards and Geoanalytical Research*, v. 34, no. 2, p. 117-134.
- Li, X. H., Qi, C. S., Liu, Y., Liang, X. R., Tu, X. L., Xie, L. W., and Yang, Y. H., 2005, Petrogenesis of the Neoproterozoic bimodal volcanic rocks along the western margin of the Yangtze Block: new constraints from Hf isotopes and Fe/Mn ratios: *Chinese Science Bulletin*, v. 50, p. 2481-2486.

- Li, X. H., Zhou, H., Chung, S. L., Lo, C. H., Wei, G., Liu, Y., and Lee, C. Y., 2002, Geochemical and Sr-Nd isotopic characteristics of late Paleogene ultrapotassic magmatism in southeastern Tibet: *International Geology Review*, v. 44, p. 559-574.
- Orihashi, Y., Maeda, J., Tanaka, R., Zeniya, R., and Niida, K., 1998, Sr and Nd isotopic data for the seven GSJ rock reference samples; JA-1, JB-1a, JB-2, JB-3, JG-1a, JGb-1 and JR-1: *Geochemical Journal*, v. 32, no. 3, p. 205-211.
- Sláma, J., Košler, J., Condon, D. J., Crowley, J. L., Gerdes, A., Hanchar, J. M., Horstwood, M. S. A., Morris, G. A., Nasdala, L., and Norberg, N., 2008, Plešovice zircon — A new natural reference material for U–Pb and Hf isotopic microanalysis: *Chemical Geology*, v. 249, no. 1, p. 1-35.
- Wei, G. J., Liang, X. R., Li, X. H., and Liu, Y., 2002, Precise measurement of Sr isotopic compositions of liquid and solid base using (LP) MCICP-MS: *Geochimica*, v. 31, p. 295-305.
- Weis, D., Kieffer, B., Maerschalk, C., Pretorius, W., and Barling, J., 2005, High-precision Pb-Sr-Nd-Hf isotopic characterization of USGS BHVO-1 and BHVO-2 reference materials: *Geochemistry, Geophysics, Geosystems*, v. 6, no. 2.
- Whitehouse, M., Claesson, S., Sunde, T., and Vestin, J., 1997, Ion microprobe U–Pb zircon geochronology and correlation of Archaean gneisses from the Lewisian Complex of Gruinard Bay, northwestern Scotland: *Geochimica et Cosmochimica Acta*, v. 61, no. 20, p. 4429-4438.
- Wiedenbeck, M., Alle, P., Corfu, F., Griffin, W., Meier, M., Oberli, F. v., Quadt, A. v., Roddick, J., and Spiegel, W., 1995, Three natural zircon standards for U-Th-Pb, Lu-Hf, trace element and REE analyses: *Geostandards newsletter*, v. 19, no. 1, p. 1-23.
- Wiedenbeck, M., Hanchar, J. M., Peck, W. H., Sylvester, P., Valley, J., Whitehouse, M., Kronz, A., Morishita, Y., Nasdala, L., and Fiebig, J., 2004, Further characterisation of the 91500 zircon crystal: *Geostandards and Geoanalytical Research*, v. 28, no. 1, p. 9-39.

# Eocene magmatism in the Himalaya: A response to lithospheric flexure during early Indian collision?

Lin Ma et al.

## Data Depository 2 (Figures)

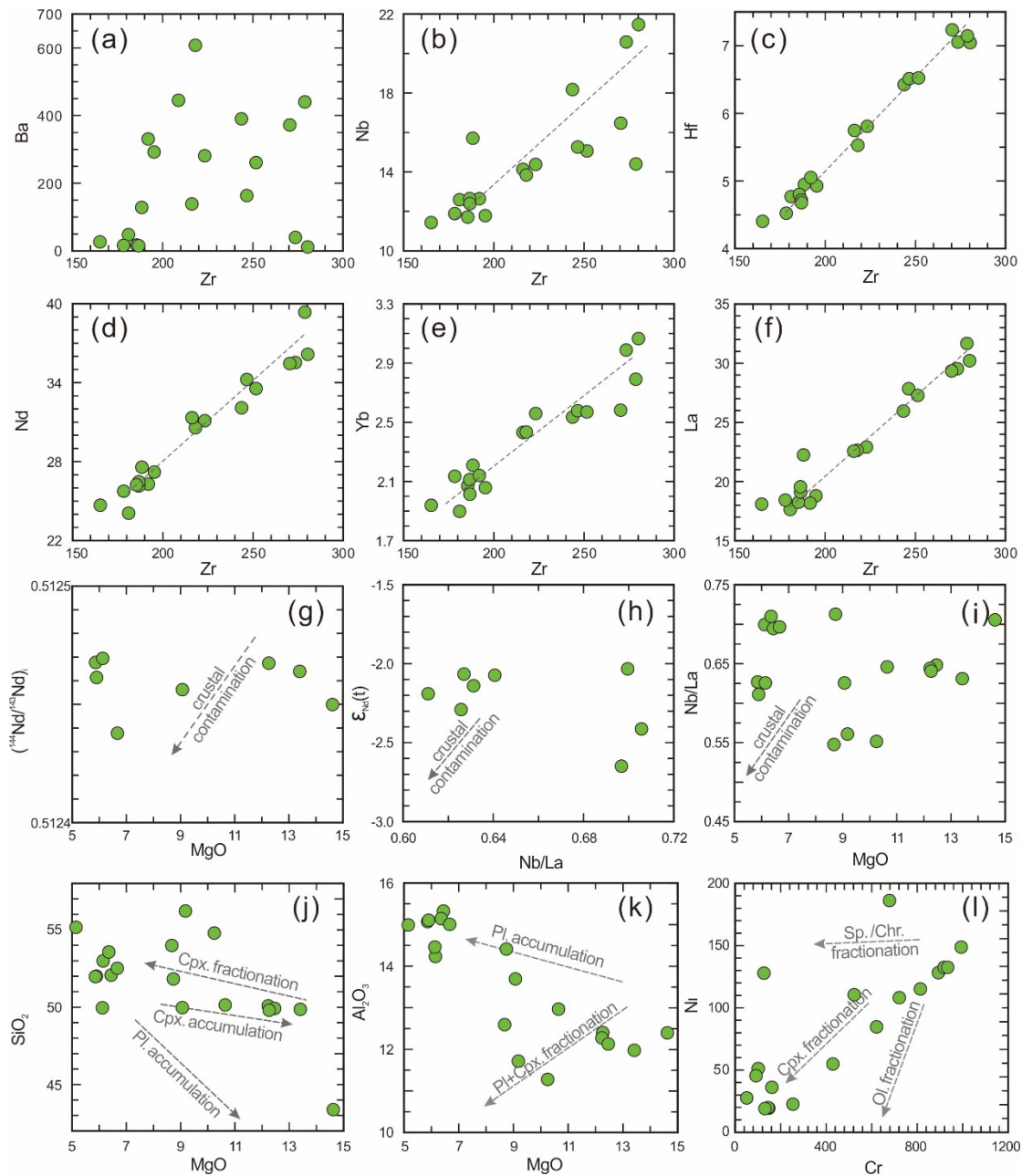


**Figure DR1** Geochemical correlation diagrams of the Gyantse dykes. Abbreviations: Sp. = spinel, Chr. = chromite, Cpx. = clinopyroxene, Ol. = olivine.



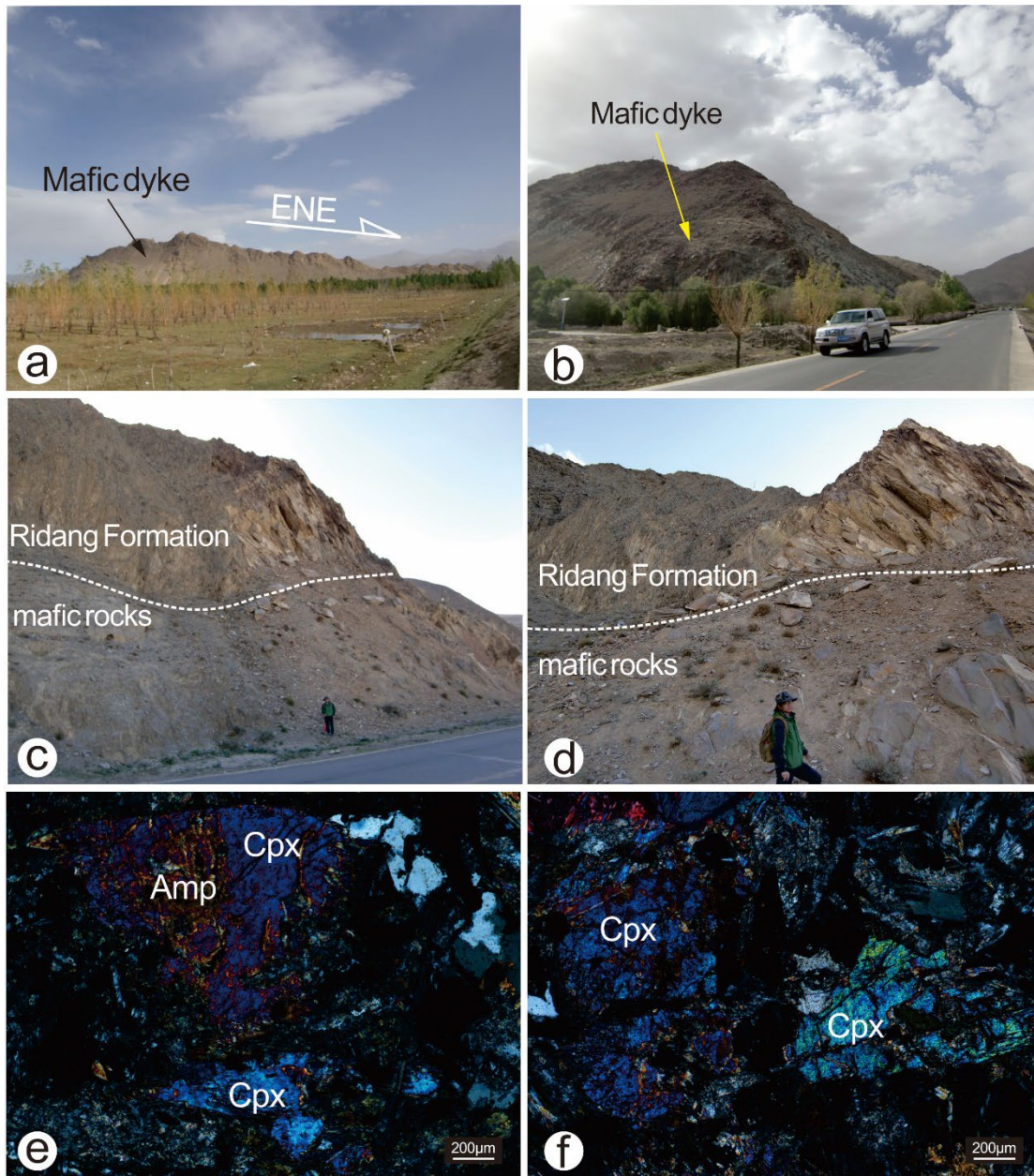


**Figure DR2** Field geological observation and petrography (plane-polarized light) of the Dagze mafic rocks: (a-b) Gyantse dykes; (c-e) mafic dykes covered by Ridang Formation limestones; (e-f) petrography of Gyantse mafic rocks. Abbreviations here: Cpx, clinopyroxene; Amp, amphibole.

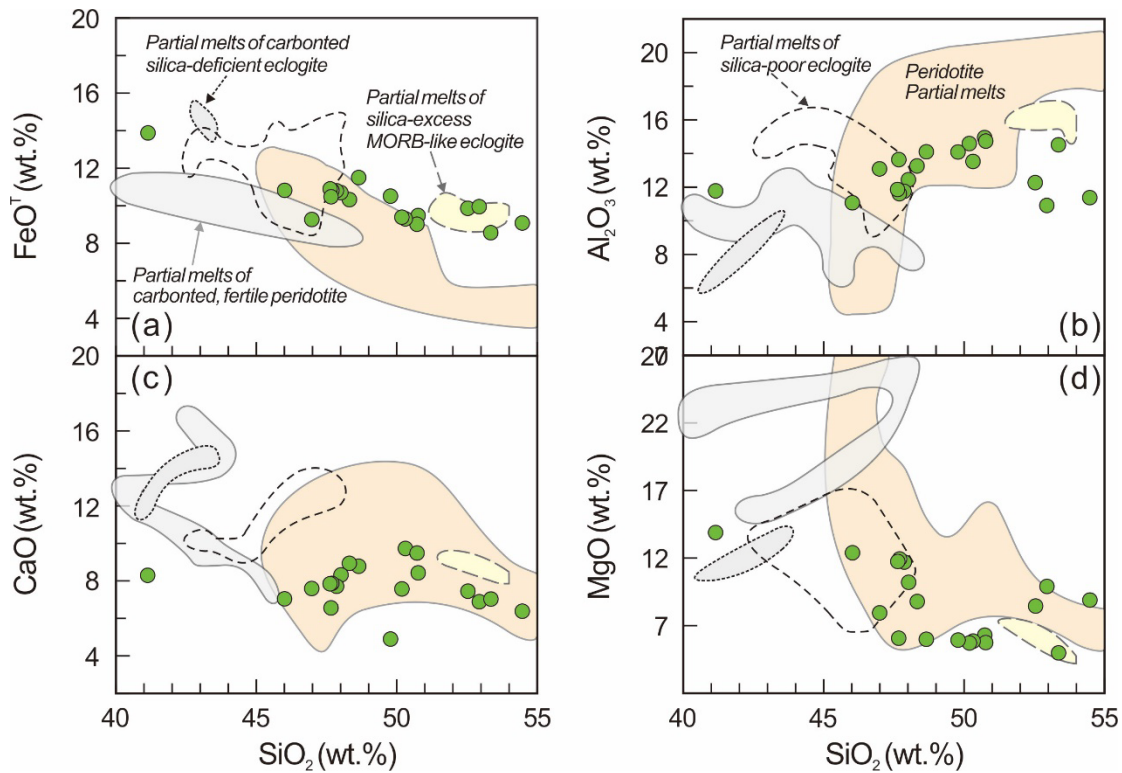


**Figure DR3** Comparison of Gyantse mafic rocks with experimental partial melts. The fields of experiment partial melts are modified from [Dasgupta et al. \(2010\)](#).

#### References Cited

Dasgupta, R., and Hirschmann, M. M., 2010, The deep carbon cycle and melting in Earth's interior: Earth & Planetary Science Letters, v. 298, no. 1, p. 1-13.